IEEE Access
Multidisciplinary ⋮ Rapid Review ⋮ Open Access Journal

Received July 23, 2021, accepted September 14, 2021, date of publication September 23, 2021, date of current version October 1, 2021.

Digital Object Identifier 10.1109/ACCESS.2021.3115142

Fighter Equipment Contribution Evaluation Based on Maneuver Decision

HANCHEN LU[1], BOYI WU[1,2], AND JUNQING CHEN[1]
[1]School of Economics and Management, Harbin Engineering University, Heilongjiang 150001, China
[2]China International Engineering Consulting Corporation, Beijing 100044, China

Corresponding author: Hanchen Lu (hidelu@yeah.net)

ABSTRACT With the development of integrated technology and equipment systems, decision-making support has been increasingly applied in equipment research and development, especially in air combat. The development of airborne equipment can significantly improve the confrontation ability of manned fighters. Contribution evaluations restrict decision making in equipment research and development and are important in beyond-visual-range (BVR) air combat, which involves dynamic and uncertain enemy positions. This paper proposes a contribution evaluation model for BVR air combat based on autonomous maneuver decision making; this approach mainly includes a situation evaluation model, a maneuver decision model, and a one-to-one BVR air combat evaluation model. However, such a model includes a high-dimensional state and action space, which require many computations, especially if equipment changes occur. Then, an autonomous maneuver decision algorithm based on the influence diagram method is proposed; this algorithm uses a rolling time domain concept to improve combat fidelity and obtain useful equipment contribution evaluation results. Finally, one-to-one BVR air combat is simulated based on different aircraft models and airborne equipment. The simulation results show that the proposed maneuver decision model and countermeasure evaluation model can help experts quantify the contributions of equipment and provide adequate decision-making support to improve equipment systems.

INDEX TERMS Equipment contribution, influence diagrams, maneuver decision, situation assessment.

I. INTRODUCTION

The development of fighter airborne equipment plays a fundamental role in national defense and security. This field has attracted considerable attention in beyond-visual-range (BVR) air combat, short-range air combat, and other air control tasks. With the continuous expansion and extension of the equipment system development strategy, equipment has gradually expanded in the context of intelligence, integration, and informatization [1]. The decision-making used in equipment research and development (R&D) has been given increased attention. Although fighter performance has been significantly improved due to the continuous development of equipment, R&D has gradually reached a bottleneck. Simply improving equipment performance cannot effectively improve the confrontation capabilities of air combat equipment systems. Therefore, the traditional R&D decision-making process cannot be used to promote the coordinated development of fighter equipment systems [2], and it is difficult to adapt to fast-changing air combat scenarios. Thus, it is necessary to evaluate whether new equipment types meet the relevant development needs from a macro perspective. Equipment contribution assessment is a significant research direction for R&D decision making and equipment development, and such assessments can provide decision support for equipment R&D projects.

Improvements to the national defense capability require changes in the development mode of equipment, from advancing technology to the coordinated development of equipment systems. Research on equipment contribution evaluation is in the initial exploration stage in China, so the contribution to equipment is the most challenging application direction in the current system construction. Equipment contribution assessments in air combat scenarios require the automatic generation of flight control instructions based on situation assessment, autonomous maneuver decisions, and other technical information to accurately reflect the impact of equipment.

The method used to calculate equipment contribution can be generally divided into three categories: system

The associate editor coordinating the review of this manuscript and approving it for publication was Ming Xu.

architecture [3]–[7], equipment capability [9]–[13] and equipment efficiency [14]–[21] methods. Representative methods based on system architecture include operation loop [3], [4], invulnerability analysis [5], [6], and complex network [7] methods. In [5], a vulnerability assessment method was used to evaluate the vulnerability of all equipment in a subway system, and reduce the failure rate of the equipment used in subway operation. In [7], in military operation planning, a complex network was used to build a capability-based analysis framework to measure the contributions of equipment and improve network flexibility. Equipment architecture refers to the interrelationships among the components of a system. A model established based on this kind of method can analyze the role of architecture in combat confrontations and reflect the contribution of equipment through architecture optimization. However, previous studies mainly focused on the decomposition and construction of evaluation indexes, and the developed methods were characterized by poor compatibility among equipment types and high computational complexity for large-scale equipment systems [8].

Equipment capability-based methods mainly include the technique for order preference by similarity to an ideal solution (TOPSIS) [9], data envelopment analysis (DEA) [10], grey correlation [11], [12] and evidence reasoning [13]. Capability evaluation can express the static attributes of an equipment system and reflect the contribution of a particular equipment type to a change in system combat capability under certain combat conditions. In [9], a vague set and the TOPSIS method were used to evaluate the contribution of an equipment system to fault reduction. In [10], the DEA method was used to evaluate the support capability of aircraft equipment, and the principal component analysis (PCA) method was introduced into the proposed algorithm for contribution evaluation and advanced aircraft support. In [12], the gray correlation method was used to model a gray entropy balance function and optimize the resolution coefficient in a comprehensive combat benefit evaluation model for fighters. In [13], an evidence reasoning method was used to construct a conditional evidence network and evaluate the contributions of weapon systems based on the relevant capability requirements by using a confidence distribution and inverse conditional confidence. The model established with this method could directly obtain evaluation indexes and was comprehensive, but it was insufficient in considering the relationships among indexes.

The equipment efficiency can be evaluated based on Bayesian networks (BNs) [14], [15], ADC (availability, dependability and capacity) [16], AHP [17], influence diagrams [18]–[21], and other methods. Equipment efficiency refers to the ability of an equipment system to achieve specific mission objectives. In this context, the concept of dynamic assessment can be introduced into benefit evaluation. In [15], with Netica software, a Bayesian network was used to perform a benefit evaluation of equipment maintenance support based on the gradient descent method for network parameter learning. In [16], to improve the efficiency of benefit analysis for a missile weapon system during the flight process, the index system and related coefficients in the ADC-based benefit evaluation model were revised and improved. In [17], the AHP method was combined with ADC to evaluate landmine combat based on a combined calculation model. Benefit evaluation can effectively identify the influences and uncertainty relationships among qualitative indexes, quantitative indexes and fuzzy indexes involved in an equipment contribution assessment. However, the problems caused by extensive data requirements must be solved.

To enhance applicability and reduce computational complexity, many scholars have performed research on influence diagrams based on algorithm improvements. In [18], fuzzy influence diagrams were used to analyze the influence of the natural battlefield environment on military combat benefits. In [19], a new type of probabilistic graphical model based on influence diagrams and a Markov decision process was used with a state transition model in a cost-benefit analysis of medicine. In [20], influence diagrams were used in combination with fuzzy multicriteria decision making theory to assess the risks of distribution network assets in uncertain environments. In [21], fuzzy evidence influence diagrams and Dempster–Shafer evidence theory were combined to obtain accurate evaluation results while reducing some calculation requirements. However, although influence diagrams are commonly used in the fields of decision making and risk assessment, previous studies did not fully and realistically consider equipment efficiency, especially when calculating contributions.

In this paper, based on influence diagrams, the BVR air combat autonomous maneuver decision model is proposed, and the killing benefit in air combat is defined to reflect the corresponding equipment contribution. First, based on the characteristics of BVR air combat, the equipment contribution concept and corresponding formulas are proposed. Five situation domains are used to simulate the driver decision process, and four situation nodes, including radar detection and missile attack nodes, are considered. Then, an air combat situation assessment model based on influence diagrams is proposed. Second, evidence-based reasoning theory is used to design a situation domain assessment method to quantitatively reflect the environmental situation in air combat. Finally, four-state advantage functions and the rolling time-domain theory are combined to design a utility structure for the maneuver decision model and calculate the killing benefit considering missile launch decisions. A comprehensive mathematical model of air combat confrontation is established to effectively improves the fidelity of confrontation state. Through a large number of machine-to-machine confrontation simulation experiments with various initial states based on the MATLAB platform [22], [23], an analysis of the maneuvering decision process is performed; the results verify that the model can autonomously output reasonable maneuvers for a certain goal and ensure high-quality results for fighter missile attack decisions and kill efficiency

calculations. The proposed dynamic method based on influence diagrams can be used to realistically assess a situation involving BVR air combat, and the superiority and killing benefit calculations are more accurate than those based on static methods; therefore, this method can accurately relate equipment contributions and the roles of equipment in a system. Moreover, with continuous improvements to system equipment, the equipment can be tested in various application scenarios.

The remainder of this paper is structured as follows. In section 2, the equipment contribution design and situation assessment model are established. The maneuver decision method based on an influence diagram model is introduced in Section 3. Section 4 includes model testing, simulation and assessments of equipment contributions. Finally, Section 5 concludes the paper.

II. EQUIPMENT CONTRIBUTION AND SITUATION ASSESSMENT MODEL

A. THE CONCEPT OF CONTRIBUTION

Combat aircraft weapon capabilities directly affect the outcome of combat missions, and different mission environments are associated with different weapon requirements; therefore, R&D is constantly needed to develop new weaponry. In modern air warfare situations, the development of weaponry is not limited to improvements in the performance of individual weapons, and applicability and economic indexes are considered in the overall construction of a weaponry system. Therefore, by analyzing the contributions of individual equipment types in aircraft combat weaponry system tasks, we can intuitively conclude whether a weapon provides positive support for air warfare tasks.

An air combat weaponry system can be used in a variety of combat scenarios, including air-to-air scenarios, air-to-ground scenarios, electronic reconnaissance and other tasks; furthermore, different combat tasks occur in a variety of environmental situations; for example, air-to-air combat includes one-to-one close combat, BVR combat, multi-aircraft cooperative combat, etc. Moreover, different mission objectives are assigned different levels of concern. Therefore, weapon contribution research must focus on the specific mission objectives. This paper uses one-to-one BVR air combat as an example for analysis.

To comprehensively analyze the ability of weaponry to contribute to a combat system, we cannot focus solely on the contribution in a static system and must consider the entire process of task completion in a given environment and the objectives of the mission. Additionally, the degree of mission completion should be considered when analyzing the contribution of a weaponry system and evaluating the actual support capability of weapon-related equipment. For a certain equipment type P_i, the corresponding contribution is calculated as shown in (1):

$$con_{P_i} = \frac{E_{P_i} - E_{non\text{-}P_i}}{E_{non\text{-}P_i}} \times 100\% \tag{1}$$

where E_{P_i} is the operational benefit of the weaponry system containing P_i and $E_{non\text{-}P_i}$ is the benefit after P_i is removed from the system [3]. When a given piece of new equipment is necessary for the operation of the corresponding combat system and cannot be removed, the ratio of the difference between the effectiveness of the combat system containing the equipment to that of the original system without the equipment can be used to measure the contribution of the new equipment in terms of capability improvement.

B. SITUATION ASSESSMENT

Since the state space of an air combat model is very large, if fighters use unprocessed situation data to make maneuver decisions, the results could be devastating, and simulations could produce a large number of invalid confrontation samples. This issue would decrease the credibility of the confrontation results, and the equipment contributions could not be accurately constrained. In response to this problem, a situation assessment method is designed for the analysis process of fighter pilots in a battlefield environment.

In this context, the proposed method divides situation assessment into three parts. First, for the BVR air combat task, the countermeasure situation is decomposed into independent states with the situation domain analysis method [24]. The corresponding condition and target are given to improve the understanding of the battlefield environment. Second, by analyzing the transformation relationship between situation domains, a situation assessment model is constructed based on the influence diagram method. The influential elements identified in a confrontation scenario correspond to the nodes in the model. Finally, after the influential node model is designed in the situation assessment model, a situation domain determination method based on the certainty factor (CF) is proposed to provide adequate information support for maneuver decisions.

1) SITUATIONAL DOMAIN

To analyze typical one-to-one BVR air combat missions, four battlefield environments are considered during the combat task, and the combat phases are start, attack, return, and defense. Through decomposition, structurally mapping and extracting the relevant elements, and analyzing the intrinsic connections among elements in a given task scenario, the four battlefield environments can be mapped into five situational domains: advantage guarantee, attack, defensive attack, defense, and information assurance. The conditions and definitions of the situational domain classifications are shown in Table 1.

The transformation of a situational domain reflects the thought process of a pilot in battle. The execution of a BVR attack mission starts with acknowledging the enemy's status, assessing the current environment and enemy information, determining the advantages and disadvantages of ally fighters, and selecting countermeasures and maneuvers based on situational information. The situational domain transformation relationship flow chart is shown in Figure 1.

TABLE 1. Situational domain classifications for BVR.

Situational Domain	Condition	Objectives
Advantage Guarantee	Distance information is available (Outside the attack area)	Gain tactical advantage
Attack	1.The enemy has not launched a missile; 2.our side has launched or can launch a missile	1. Successfully launch own missiles; 2. create conditions for enemy missiles to be difficult to launch
Defensive attack	1.Enemy has launched; 2. our side has launched a missile or can organize return fire	1.Effective defense against enemy missiles; 2.Successfully launch own missiles
Defense	1.Enemy has launched; 2.own side has not fired missile and cannot return fire	1.Effective defense against enemy missiles; 2. maintaining the possibility of continued attack
Information Assurance	No assessment of objectives	Guaranteed fastest access to information

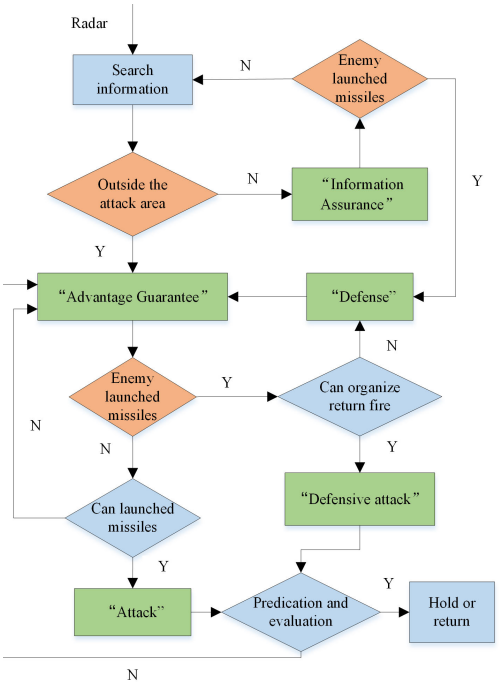

FIGURE 1. Situational domain interrelationship diagram.

2) SITUATION ASSESSMENT MODEL

The construction of a model requires qualitative and quantitative descriptions of the relevant intra-system situation assessment components, including the elements of the situational environment and the interrelationships among factors that influence BVR air combat tasks. The influence diagram method is chosen for modeling based on existing research; it, on the one hand, can visually and effectively express the internal relationships among evaluation components and, on the other hand, is normative and efficient decision analysis approach that yields good performance in both situation assessment and maneuvering decision making [25].

An influence diagram can describe an equipment contribution model with a probabilistic network structure and a utility structure. The situation assessment is based on a Bayesian network for numerical analysis, and probabilistic determination analysis is performed through the probabilistic network structure and influence diagram. The utility structure is used for maneuver decision calculations in the confrontation system. Influence diagrams without decision nodes and value nodes can be considered Bayesian networks [26], and based on the normative influence diagram description method, an influence diagram for situation assessment can be constructed as shown in Figure 2.

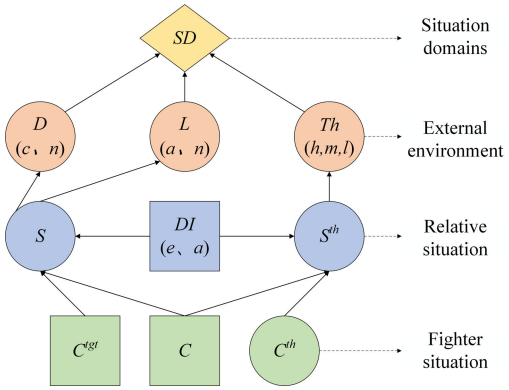

FIGURE 2. Situational domain determination diagram.

As shown in the Figure 2, situational domain determination in situation assessment focuses on three main scenarios involving a given fighter and the enemy: whether the enemy aircraft is within radar range; whether the enemy aircraft is a threat to attack, and whether we can launch an attack against the enemy aircraft [27]. The data are derived from the status node C, enemy status node C_{tgt} and threat status node C_{th} based on the battlefield positions of the fighter and enemy fighter. Based on this situational relationship approach, the nodes in the situation influence diagram and related factors are shown in Table 2.

TABLE 2. Descriptions of the BVR situation assessment nodes.

Node	Definition	Output category
SD	Situational domain	*atk*- attack, *dfc*- defense *atk_dfc*- defensive attack *grtadv*- Advantage Guarantee *grtinf*- Information Guarantee
D	Enemy detection status	*c*-Target detectable *n*-Target undetectable
L	Missile launch status	*a*- The missile can be launched *n*- The missile cannot be launched
Th	Missile threat status	*h*- high threat, *m*- medium threat *l*- low threat
DI	Interfering status	*e*-Environmental interference *a*-Active interference
S	Relative situation	Status parameters
Sth	Threat situation	Status parameters

C. SITUATION NODES

Based on the node design approach used in the situation assessment influence diagram, situational domain calculations require numerical structural descriptions of the radar

detection node D, missile attack node L and enemy aircraft threat node Th.

1) RADAR DETECTION NODE D

The main variables of interest for radar detection nodes are the maximum radar search azimuth φ_R, maximum radar search distance D_R, and radar detection probability P_{Rdect} [28]. The parameters associated with node R are D_{Mmax} related to the performance of the airborne radar sensor. The node operation scenario assumes that the friendly aircraft is guided to the enemy aircraft by a ground base station or an early warning aircraft, and is within the effective detection range of radar; thus, the radar detection probability can be defined as

$$P_{Rdect} = (\varphi_R/360) \times P_{Tgtdect} \tag{2}$$

where $P_{Tgtdect}$ is the probability of an enemy aircraft being detected by radar, the calculation of which depends on the RCS (Radar Cross-section) area of the enemy aircraft; an enemy target with an RCS of $5m^2$ is used as an example [29]. The probability of detection at a distance of d can be defined as

$$P_{Tgtdect} = e^{(-0.1625d/D_R)} \tag{3}$$

For a radar detection node R in different situational environments, the node status can detectable c or undetectable n, and the corresponding probability distribution Π_R can be defined as $P(c|D) = P_{Rdect}$ and $P(n|D) = 1 - P_{Rdect}$.

2) MISSILE ATTACK NODE L

A missile attack node determines whether the enemy aircraft falls into the missile launch envelope based on its relative position at the moment of launch. The node state is simplified to a launchable missile state a or a non-launchable state n. The corresponding membership function is defined as

$$P(a|L) = \begin{cases} 1 & D_{Mmin} \le d \le D_{Mmax}, \ |\theta| \le \varphi_M \\ 0 & d < D_{Mmin} | d > D_{Mmax}, \ |\theta| > \varphi_M \end{cases} \tag{4}$$

$$P(n|L) = 1 - P(a|L) \tag{5}$$

The main variables considered by a missile attack node are the maximum off-axis launch angle of the missile φ_M, the maximum/minimum attack range $D_{Mmax}/D_{M\,\min}$, and the maximum/minimum inescapable range $D_{Mkmax}/D_{Mk\,\min}$, where D_M is the missile launch envelope. The ''no escape zone'' is an area in which no matter what kind of maneuvering the target performs in the available overload range, a missile will damage the target when launched in this area [30]. A plot of changes in the missile launch envelope is shown in Figure 3. According to the simulation in [31], in tail pursuit, the boundary of the missile attack zone and the boundary of the no-escape zone coincide. At this time, as long as the enemy aircraft is within the attack range, it cannot escape; that is, $D_{Mmax} = D_{Mkmax}$.

In this paper, for convenience, only the changes in the aircraft azimuth ω and entry angle θ at the moment of missile launching are considered. From the analysis of the factors that influence the long-range air-to-air missile attack range, when an air-to-air missile is in the horizontal plane ($\omega = 0$, $\theta = 180^{o}$), the launching range of the missile is maximized and can be approximately regarded as an ellipse [32]. The semi-major axis and semi-minor axis of the current state transmission envelope are defined as a and b, respectively. The maximum attack range function is

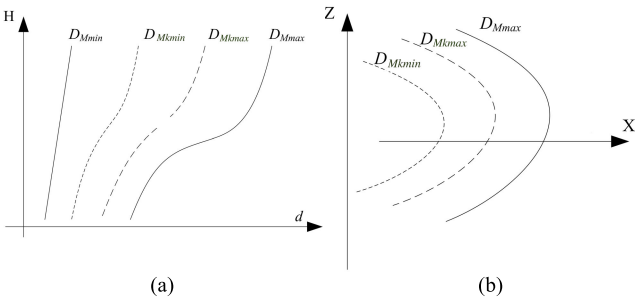

FIGURE 3. Relationship between the missile launch envelope and inescapable range (a: Vertical section, b: horizontal section).

$$D_{Mmax} = \frac{a}{2 - \cos\omega} - b\cos\theta \tag{6}$$

3) ENEMY AIRCRAFT THREAT NODE TH

The main variables of interest for enemy fighter threat nodes are the maximum airborne radar detection distance D_{dectM}, maximum attack range D_{Mmax}, RCS, target detection probability P_{Rdect}, and radar interference resistance factor I_R. The objective of BVR air combat is to achieve a state of superiority by firing before the enemy; therefore, an enemy fighter threat node considers the probability of an ally fighter firing missiles before an enemy fighter. The prior launch index A is calculated as

$$A = \ln\left(\frac{D_{dectM} \cdot D_{Mmax} \cdot P_{Rdect} \cdot I_R}{RCS^{0.25}}\right) \tag{7}$$

In the course of combat, the friendly aircraft calculates the a priori launch indexes of both aircraft according to the current situation parameters A_{atk} and A_{tgt}. When $A_{atk} > A_{tgt} \ge 0$, the performance of the ally aircraft is better than that of the enemy aircraft, and the enemy aircraft threat probability distribution can be defined as

$$P(h|Th) = P_{Th} = 0.5 + 0.5\left(1 - \frac{A_{tgt}}{A_{atk}}\right)^{0.5} \tag{8}$$

$$P(l|Th) = 1 - P(h|Th) \tag{9}$$

4) INTERFERENCE NODE DI

To create a situation similar to an actual BVR air combat confrontational state, an interference model is included in the situation assessment design stage, and it includes environmental interference DI_e due to weather conditions (rainfall, fog, etc.), which can affect the radar detection range of aircraft, and active interference DI_a to be actively released to reduce the detection range of the enemy's radar. The equation

for the radar detection distance considering environmental interference [33] is

$$DI_e = D_{dectM} e^{-0.0115 M_1 d} \tag{10}$$

where M_1 is the atmospheric radio wave energy absorption coefficient (Db/km) and d is the straight-line distance between the ally and enemy (km). When there is active interference in the confrontation environment and the spectral density of the interference signal is greater than 0.1, the target detection range can be defined as

$$DI_a = (D_{dectM})^{0.5} \left[\frac{A_1 * d^2}{(4\pi)^2 A_2} \right]^{0.125} \tag{11}$$

where d is the straight-line distance between the interference providing aircraft and the enemy aircraft (km); A_1 is the signal spectral density of the detection radar (W/MW); and A_2 is the spectral density of the airborne interference signal (W/MW).

D. SITUATIONAL DOMAIN DETERMINATION

By establishing an assessment model to determine the situational domain determination structure, the probability values of the nodes can be transformed into a fuzzy expert system to obtain an analytical solution based on influence diagrams. Accurate calculations based on Bayes' theorem require the probability values associated with antecedent nodes. However, in the actual calculation process, it is extremely difficult to determine the probability values of all relevant nodes and to ensure mutual consistency among nodes. Therefore, to enhance the credibility of the situation assessment results, CF is introduced to reflect the node state uncertainty. The rule used in the fuzzy expert system is

$$\text{IF } E \text{ THEN } H \text{ with } (\text{CF}(H, E) = \sigma) \tag{12}$$

CF is the determinant for state H provided that state E exists, and any way of matching is a certain value of determinant state. All the matching rules in a reasoning system can be activated with a trigger mechanism, and the state with the maximum CF value σ is the most likely situation to be encountered. The matching degree of the reasoning antecedent E for an uncertain event e is represented by the CF of the reasoning antecedent $CF(E, e)$. All rules need to be activated by setting the threshold β of the antecedent $CF(E, e)$. If $CF(E, e) > \beta$ is satisfied, the antecedent of the rule is determined to match, and the rule is in an active state [34]. In this regard, the certainty factor can be defined by the uncertain fact e as $CF(H, e) = CF(E, e)CF(H, E)$.

When the antecedent of a rule involves certainty, the result is given as a conditional probability $P(H|E) = \sigma$; conversely, when the antecedent of a rule involves uncertainty, then $CF(E, e)$ corresponds to the probability $P_E(e)$. This approach is combined with the constructed situation assessment model base on influence diagrams, and situational domain determination nodes SD can be expressed as situational domain probability values corresponding to the Th, D, and L nodes for different situations $P(Fd|Th, D, L)$. For nodes Th, D, and L corresponding to states h, c, and a, respectively, the CF of the antecedent E can be calculated as

$$CF(E, e) = \min[CF(Th, h), CF(D, c), CF(L, a)] \tag{13}$$

The threshold β is used to determine whether a rule is triggered or not. However, in the process of using fuzzy methods, the same reasoning result may be triggered by different rules at the same time. Therefore, for a reasoning calculation with multiple CFs, the combined function set is established as

$$CF_{comb}(CF_1, CF_2) = \begin{cases} CF_1 + CF_2(1 - CF_1) & CF_1 > 0,\ CF_2 > 0, \\ \dfrac{CF_1 + CF_2}{1 - \min(|CF_1|, |CF_2|)} & CF_1 | CF_2 < 0 \\ CF_1 + CF_2(1 + CF_1) & CF_1 < 0,\ CF_2 < 0 \end{cases} \tag{14}$$

An iterative calculation is used for this function set, and the first step is to calculate the CF_{comb} values for any two rules. The second step is to calculate the initial CF_{comb} and the CF for the next rule in combination until all the triggered rules are considered. Through this method, the CF combinations of the five situational domains are based on information from three nodes Th, L, and D with different state combinations. The maximum CF_{comb} is the final result of the proposed situation assessment method.

III. MANEUVER DECISION-MAKING METHOD

Because many factors influence BVR air combat, the confrontation process is quite different from that in actual air combat if the fighter's maneuvering strategy is not well designed. The credibility of the simulation results will be significantly reduced in such cases because the actual impact of available equipment is not accurately known. In response to this problem, a maneuver decision-making method for BVR air combat missions is designed based on the attributes of the situation domain.

First, a situation domain is input into the model. Combined with the three-dimensional particle model of a fighter, the maneuver decision model is constructed based on influence diagrams. The model transforms the process of maneuver decision making into a utility structure to generate the optimal maneuver strategy by predicting enemy maneuvers. Second, a benefit function is designed for nodes in the utility structure. A fighter can use the best maneuvering strategy and attack strategy at the current moment and defeat a target in BVR air combat.

A. AIRCRAFT MOTION MODEL

In Figure 4, the ally fighter is shown in red, and the enemy fighter is shown in blue; the relationship between the two aircraft during a confrontation is depicted. At any moment k, the state of the enemy and the ally I is described as $C_k^i = [x_k^i, y_k^i, h_k^i, \gamma_k^i, \chi_k^i, v_k^i]^T$.

where $i = R, B$. Each vector includes the 3D position coordinates x, y, and h of the aircraft, the track angle, the heading angle, and the velocity. u_k^i is set as the control vector for

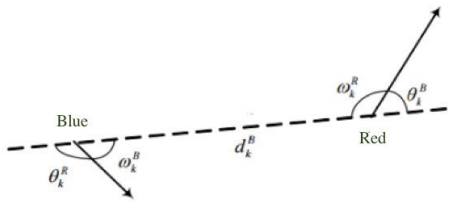

FIGURE 4. BVR situation.

the aircraft. To approximate the pilot control mode, the aircraft angle of attack control α_k^i is represented by the normal acceleration for overload n_x. The throttle stick position η_k^i is represented by the tangential acceleration for overload n_y, and lateral overload control is derived from the aircraft traverse angle μ_k^i [35]. The control vector is recorded as $u_k^i = [\alpha_k^i, \eta_k^i, \mu_k^i]^T = [n_x^i, \eta_y^i, \mu_k^i]^T$. The state vector of the fighter at a given moment can be defined as

$$C_{k+1}^i = C_k^i + \int_{t_k}^{t_{k+1}} f^i(C_k^i, u_k^i)dt \tag{15}$$

The focus of this paper is implementing BVR countermeasures through maneuver decision making considering the contributions of airborne equipment. This process mainly considers the positional relationship between aircraft and the corresponding aircraft velocity vectors in three-dimensional space. To simplify the analysis process, a three-degree-of-freedom particle point model was used as the aircraft motion model, as shown in (16), and the dynamic model of the aircraft is shown in (17). According to the aircraft motion model, the relative situation between an enemy and ally in the battlefield environment is shown in (18).

$$\begin{aligned}
\dot{x} &= v\cos\gamma\cos\chi \\
\dot{y} &= v\cos\gamma\sin\chi \\
\dot{h} &= v\sin\gamma \\
\dot{\gamma} &= \frac{g}{v}(n_y\cos\mu - \cos\gamma) \\
\dot{\chi} &= \frac{gn_y\sin\mu}{v\cos\gamma}
\end{aligned} \tag{16}$$

$$\dot{v} = g(n_x - g\sin\gamma) \tag{17}$$

$$S_k^i = S^i(X_k^R, X_k^B) = [d_k^i, d_h, \Delta d, \omega_k^i, \theta_k^i, v_k^i] \tag{18}$$

The situation formula includes the straight-line distance, horizontal distance, altitude difference, azimuth, angle of entry and velocity difference between the enemy and ally aircraft. With the enemy (blue aircraft) as an example, the azimuth, angle of entry, and distance between the two aircraft are calculated as shown in (19).

$$\begin{aligned}
\omega_k^B &= \arccos\{[(x_k^R - x_k^B)\cos\gamma_k^B\cos\chi_k^B \\
&\quad + (y_k^R - y_k^B)\cos\gamma_k^B\sin\chi_k^B + (h_k^R - h_k^B)\sin\gamma_k^B]/d_k^B\} \\
\theta_k^B &= \arccos\{[(x_k^R - x_k^B)\cos\gamma_k^R\cos\chi_k^R \\
&\quad + (y_k^R - y_k^B)\cos\gamma_k^R\sin\chi_k^R + (h_k^R - h_k^B)\sin\gamma_k^R]/d_k^B\} \\
d_k^B &= \sqrt{(x_k^R - x_k^B)^2 + (y_k^R - y_k^B)^2 + (h_k^R - h_k^B)^2}
\end{aligned} \tag{19}$$

B. THE UTILITY STRUCTURE

The maneuver decision method establishes a utility structure in terms of an influence diagram approach with the current air combat situational domain state as the input and a maneuver as the output, as reflected by the influence diagram structure shown in Figure 5. The node *Vc* for a fighter maneuver consists of multiple value nodes that are interlinked, and the inputs are the current situations of the ally C and target C_{tgt}, the missile attack situation C_{th}, and the situation assessment result *SD*. The constituent decision nodes include the maneuver library *Mn*, missile launch state *Fm*, hit estimate for a missile *FD*, active interference release state *Ri*, and estimate of the enemy escape state *EJ*. Detailed descriptions of nodes are given in Table 3.

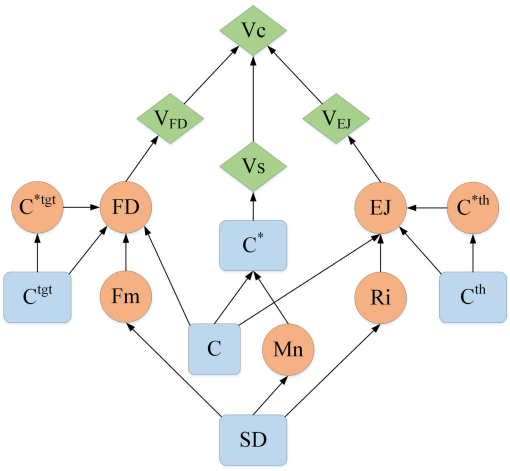

FIGURE 5. Influence diagram for the maneuver decision model.

TABLE 3. Descriptions of the BVR influence diagram nodes.

	Definition	Output category
SD	Situational domain	*atk, dfc, atk_dfc, grtadv, grtinf*
Mn	Vertical Maneuver	*h*-hold, *c/d*- Maximum angle of attack change rate ascend / descend
	level maneuver	*h*-hold, *tl/tr*-maximum tilt angle change rate left turn/right turn
	Throttle lever operation	*m*-hold, *h/l*- Maximum rate of change increase / decrease thrust
Ri	Active interference release	*n*- no release, *f*-release radar decoy
Fm	Missile attack	*f*-launch(missile), *n*- Unable to launch (missile)
EJ	Enemy escape prediction	*f*- escape, *n*- inescapable
FD	Missile hit estimation	*h*-hit, *n*-no hit

The contribution model is designed based on the receding horizon concept in the overall algorithm layer; this approach differs from the static influence approach, and the system dynamically simulates BVR air combat. Each operation from situation assessment to maneuver decisions is associated with a given time segment in the overall air combat scenario. Calculations are performed to select the appropriate maneuver plan according to the current situational domain and determine the best maneuver by predicting the enemy and

ally situations after executing the maneuver plan. The rolling horizon concept is shown in Figure 6.

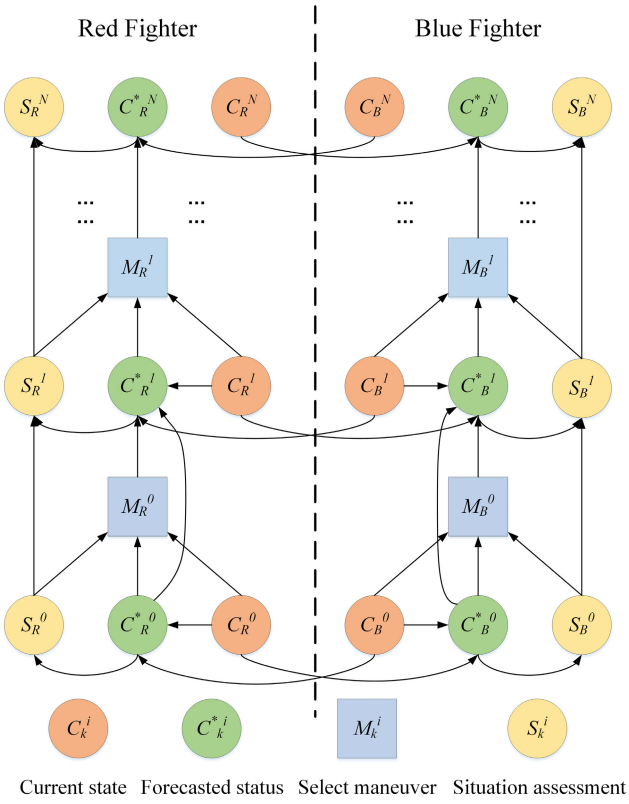

FIGURE 6. Rolling horizon approach for BVR air combat.

A maneuver is made based on a situational assessment of the current environmental situation, and the best maneuver for future situations is determined through a decision prediction algorithm. The situational domain determination and maneuver decision processes are repeated until the task is completed or the time limit is reached [36].

C. MANEUVER DECISION MODELING WITH INFLUENCE DIAGRAMS

1) DESIGN OF A BENEFIT FUNCTION

As shown in Figure 5, the benefit value of the final value node V_c in the influence diagram structure for BVR confrontation scenarios is affected by the decision scheme selected and the environmental situation. The final value node is decomposed based on corresponding benefit values in the proposed utility structure: situation benefit V_s, enemy threat benefit V_{EJ}, and missile attack benefit V_{FD}. The benefit value of node V_c can be calculated as

$$\begin{aligned} &E[\mathrm{V}_C|\mathrm{V}_S, \mathrm{V}_{EJ}, \mathrm{V}_{FD}] \\ &= \omega_{FD} E[\mathrm{V}_{FD}|\mathrm{FD}] \\ &\quad + \omega_S E[\mathrm{V}_S|\mathrm{C}, \mathrm{C}^{\mathrm{tgt}}] + \omega_{EJ} E[\mathrm{V}_{EJ}|EJ] \end{aligned} \tag{20}$$

where ω is the weight coefficient set for the value nodes. The weight coefficient is set based on the degree of attention given to different node values. Further decomposition can be performed for sub-functions, such that the situation benefit function S is related to the energy advantage V_s and position advantage V_P; additionally, the energy advantage depends on the aircraft velocity v and height h. The positional advantage depends on the relevant distance dis, azimuth φ and angle of entry θ values. In conclusion, the situation benefit function S is shown in (22):

$$\begin{aligned} E[\mathrm{V}_S|\mathrm{C}, \mathrm{C}^{\mathrm{tgt}}] &= E[\mathrm{V}_E|\mathrm{C}, \mathrm{C}^{\mathrm{tgt}}] + E[\mathrm{V}_P|\mathrm{C}, \mathrm{C}^{\mathrm{tgt}}] \\ &= \alpha_1 f_1(v) + \alpha_2 f_2(h) + \beta_1 f_3(dis) \\ &\quad + \beta_2 f_4(\phi) + \beta_3 f_5(q) \end{aligned} \tag{21}$$

where $\alpha_1 + \alpha_2 = 1$ and $\beta_1 + \beta_2 + \beta_3 = 1$.

2) ADVANTAGE FUNCTION

For the selection of the three coefficients ω, α and β, it is necessary to consider the various conditions pilots encounter in real air combat, collect and analyze combat experience information, and determine the physical and psychological conditions of different pilots in confrontations. To effectively simulate the pilot decision process during air combat operations, different air combat situations and task objectives are used to determine coefficient weights based on expert knowledge and pilot experience. A situation benefit function can be decomposed into a combination of advantages for four factors: the azimuth T_ω, entry angle T_θ, relative distance T_{dis} and energy T_e. The corresponding functions are constructed as shown in Table 4.

To simplify the calculation process, some of the functions are designed under specific conditions while meeting the computational needs for a given situation. For example, an azimuth advantage ensures that the attack conditions are better for an ally aircraft than for the enemy; the entry angle advantage enhances the kill capability of missiles; the relative distance advantage maximizes the kill probability of missiles; and the energy advantage enhances the launch range and flight speed.

3) MISSILE HIT BENEFIT AND LAUNCH DECISIONS

In terms of both the enemy and selected aircraft in a confrontational environment, the missile hit benefit is related to the kill probability P_{kill} of a missile. This paper relies on simulations and expert experience to derive the missile kill probability, which is related to numerous environmental factors, such as the parameters of the two aircraft, the relative distance between aircraft, the initial kinetic energy of the aircraft and the angle of entry of the missile, as denoted in (22) and (23).

$$P_{kill} = P_{kill}(d) \cdot P_{kill}(\theta) \tag{22}$$

$$P_{kill}(d) = \begin{cases} 0.6^{\frac{d - D_{Mkmax}}{D_{Mmax} - D_{Mkmax}}} & D_{Mkmax} \le d < D_{Mmax} \\ 1 & D_{Mkmin} \le d < D_{Mkmax} \\ 0 & else \end{cases}$$

TABLE 4. Four advantage functions.

Azimuthal	Enter the angular	relative distance[29]	Energy
$T_\omega = \begin{cases} 0 & \lvert\omega\rvert > \varphi_R \\ 0.3(1-\frac{\lvert\omega\rvert-\varphi_M}{\varphi_R-\varphi_M}) & \varphi_M \le \lvert\omega\rvert \le \varphi_R \\ 0.8-\frac{\lvert\omega\rvert-\varphi_{Mk}}{2(\varphi_M-\varphi_{Mk})} & \varphi_{Mk} \le \lvert\omega\rvert < \varphi_M \\ 1-\frac{\lvert\omega\rvert}{5\varphi_{Mk}} & 0 \le \lvert\omega\rvert < \varphi_{Mk} \end{cases}$	$T_\theta = \begin{cases} \frac{\lvert\theta\rvert}{50} & \lvert\theta\rvert < 50° \\ 1-\frac{\lvert\theta\rvert-50}{130} & 50° \le \lvert\theta\rvert < 180° \end{cases}$	$T_{dis} = \begin{cases} 0 & d \ge D_R \\ 0.5e^{-\frac{d-D_{Mmax}}{D_R-D_{Mmax}}} & D_{Mmax} \le d < D_R \\ 2^{-\frac{d-D_{Mkmax}}{D_{Mmax}-D_{Mkmax}}} & D_{Mkmax} \le d < D_{Mmax} \\ 1 & D_{Mkmin} \le d < D_{Mkmax} \\ 2^{-\frac{d-D_{Mkmin}}{10-D_{Mkmin}}} & 10 \le d < D_{Mkmin} \end{cases}$	$Eg = h + \frac{v^2}{2g}$, $T_e = \frac{Eg-Eg^{tgt}}{Eg}$

$$P_{kill}(\theta) = \begin{cases} 0 & |\theta| > \varphi_M \\ 0.2^{\frac{d-\varphi_{Mk}}{\varphi_M-\varphi_{Mk}}} & \varphi_{Mk} \le |\theta| \le \varphi_M \\ 1 & |\theta| < \varphi_{Mk} \end{cases} \tag{23}$$

If the selected fighter launches a missile at time t during a confrontation, to determine whether to stop the attack or continue to launch missiles, it is necessary to calculate the comprehensive kill probability of all the launched missiles and the overall kill benefit compared to that of the enemy; therefore, it is necessary to consider the flight state parameters of the launched missiles at time t. The correlation function constructed considering time is

$$P'_{kill}(t) = \begin{cases} 0.5P_{kill}\left(1+\cos\left(\frac{t-\tau}{\tau_m}\right)\right) & t \le \tau+\tau_m \\ 0 & t > \tau+\tau_m \end{cases} \tag{24}$$

where P_{kill} represents the initial kill probability of the launched missile, τ represents the time of the impending missile attack, and τ_m represents the flight time when the missile is launched. Based on the above considerations, the comprehensive killing effect of launching two missiles at an enemy can be defined as

$$\begin{aligned} E_{FD} = {} & \max[P'_{kill_1}, P'_{kill_2}] \\ & + (1 - \max[P'_{kill_1}, P'_{kill_2}]) \\ & \cdot \min[P'_{kill_1}, P'_{kill_2}]^{\max[P'_{kill_1}, P'_{kill_2}]} \end{aligned} \tag{25}$$

When more than two missiles have been launched, the comprehensive benefit is iteratively calculated for all missiles. Both enemy and ally pilots must determine whether to attack based on the launch conditions. The launch determination principles are shown in Table 5. E_h^{low} and E_h^{high} correspond to the low and high thresholds for missile threats, respectively, and are set to $E_h^{low} = 0.3$ and $E_h^{high} = 0.7$ in this study.

TABLE 5. Launch principles.

IF		THEN
Pre-launch Killing benefit	Post-launch Killing benefit	
$E_h^n < E_h^{low}$	$E_h^f \ge E_h^{low}$	$Fr = f$
	$E_h^f < E_h^{low}$	$Fr = n$
$E_h^{low} \le E_h^n < E_h^{high}$	$E_h^f - E_h^n \ge 0.2$	$Fr = f$
	$E_h^f - E_h^n < 0.2$	$Fr = n$
$E_h^{high} \le E_h^n < 0.95$	$E_h^f \ge 0.95$ $E_h^f - E_h^n \ge 0.1$	$Fr = f$
	$E_h^f < 0.95$	$Fr = n$
$E_h^n \ge 0.95$		$Fr = n$

IV. SIMULATION AND ANALYSIS

A. PARAMETER SETTING

Through contribution model analysis, situation assessment, and maneuver decision evaluation, this paper builds a BVR air combat countermeasure system for assessing the contributions and capabilities of weaponry. Two kinds of fighters are considered in the air combat system, and from the literature, the fighter models are constructed based on the performance indexes of F-16 and Su-27 aircraft; the corresponding control parameters are restricted as shown in Table 6. To verify the contribution of a weapon, two missiles and two airborne radar systems are considered in the countermeasure system; the detailed parameters of the system are shown in Table 7. The action space contains seven basic maneuver actions that were proposed by NASA [37]. The control values of the basic actions in the maneuver library are shown in Table 8.

In the process of BVR air combat simulation, the decision period T is set to 1 s. In typical air combat simulations, if a fighter kills the other fighter or the time threshold $T_{\max}$ is reached, the simulation will end. Next, the effectiveness of the simulation system is verified in a test with target drone attacks. Finally, the contributions of different airborne equipment types are analyzed based on autonomous decision maneuvers.

B. MODEL VALIDATION AND SIMULATION

1) TARGET DRONE TESTING

To validate the ability of the air combat system to react to real confrontations, a typical BVR scenario is selected

TABLE 6. Restrictions on aircraft control parameters.

Side		ω_f^i.deg	θ_f^i.deg	$h_f^i.m$	$d_f^i.m$	$n^i.g$	$\Delta n^i.g.s^{-1}$	$\Delta\mu^i$ deg$.s^{-1}$	$\Delta\eta^i.s^{-1}$
Blue	*S-27*	30.0	60.0	1000.0	1000.0	9	1	60.0	1.0
Red	*F-16*	30.0	60.0	1000.0	1000.0	9	1	20.0	0.5

TABLE 7. Radar and missile system parameters.

	φ_R^i.deg	$D_R^i.km$		φ_M^i.deg	φ_{MK}^i.deg	$D_{M\max}^i.km$	$D_{MK\max}^i.km$
RadarF	12.0	10.0	*MissileA*	70.0	30.0	12.0	8.0
RadarS	17.0	12.0	*MissileR*	70.0	30.0	11.0	7.0

TABLE 8. Maneuver library.

No.	maneuver	control values		
		n_x	n_y	μ (Angle)
1	left turn	0	0.005	-40
2	right turn	0	0.005	40
3	upward	2.5	1	0
4	downward	-2	1	0
5	maintain	0	1	0
6	increase thrust	0	3	0
7	decrease thrust	0	-1	0

for validation. In this case, the selected fighter uses influence diagram-based situation assessment and maneuvering decision information to establish control commands, and the target drone maintains a uniform and straight flight path.

Initial state of the selected aircraft: north, up, and east (NUE) coordinates (1000, 10000, and 4000 m) are used, and the initial direction of travel is due east. The initial attitude of the flight is level, and the flight speed is 200 m/s.

Initial conditions of the target drone: NUE coordinates (1000, 1000, and 10000 m) are used, and initial direction of flight is due north. The initial attitude of the flight is level, and the flight speed is 180 m/s.

Figure 7 gives the trajectories of the selected aircraft and the target drone, and Figure 9 shows when the fighter enters and exits the advantage guarantee and attack phases (the two aircraft are close in terms of distance, so the information guarantee phase can be ignored). The changes in maneuvers are shown in Figure 8, and the missile attack process is illustrated in Figure 10.

The maneuver decision curve in Figure 8 shows that the target drone maintains the set course at a constant speed, and the selected aircraft reaches the attack state from the advantage guarantee state and continues to increase its altitude and thus energy advantage through making reasonable decision maneuvers. By constantly performing turning maneuvers and adjusting its azimuth based on the conditions of the attack state demand, the aircraft adopts a "tail chasing-coaxial launch" tactic.

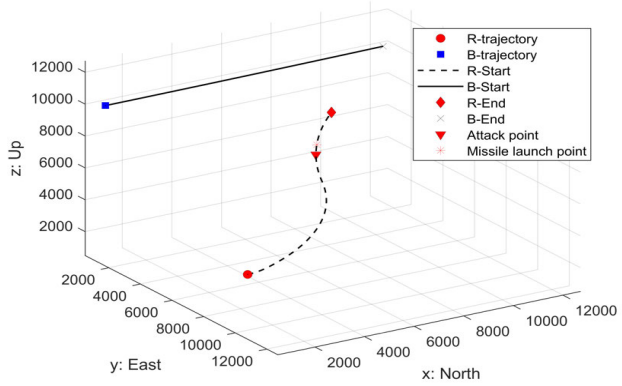

FIGURE 7. 3D view of the maneuvering trajectory in air combat (R-selected aircraft, B-target drone).

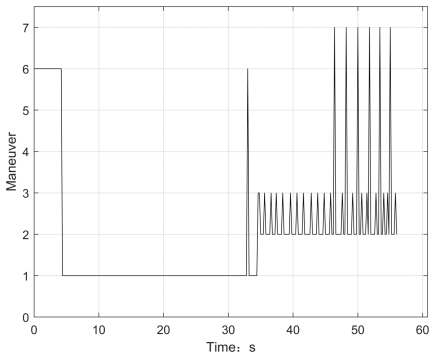

FIGURE 8. Maneuver decision changes in the process of attacking a target drone (7 maneuvers).

At 18 seconds, the fighter shifts to an operational attack state and keeps climbing with turning maneuvers to enter a tail chase state and increase the kill probability of a missile.

A launch state is reached at 42 seconds, and one missile is launched. After the launch, the destruction probability of the missile is determined to be 0.61, which is below the set destruction threshold. Thus, the aircraft remains in the launching state and launches a second missile at 55 seconds. The comprehensive kill probability of the two missiles is 0.793, which exceeds the set destruction threshold; thus, the damage task is complete. The simulation results highlight

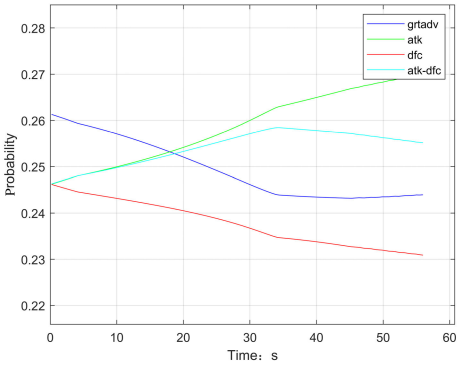

FIGURE 9. Probability changes in four situation assessments.

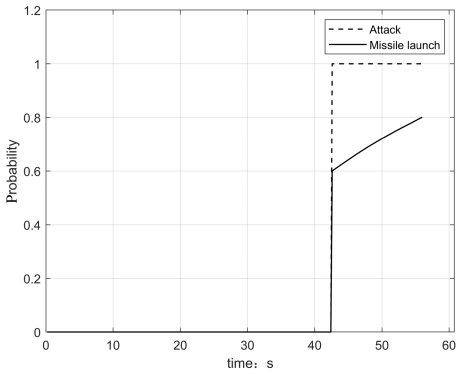

FIGURE 10. Missile kill probability and launch determination (based on launch principles, as shown in Table 5).

the validity and feasibility of the proposed model and algorithm.

2) CONFRONTATION SIMULATION

In this simulation, both the enemy and selected aircraft use autonomous maneuvering decisions during a confrontation, and either side could complete a destruction task. The change in kill benefit is used to calculate the equipment contributions. In the initial battlefield environment, the selected aircraft is in a better situation than that of the enemy, and the initial situation conditions are shown in Table 9. To avoid a confrontation that cannot be ended because the same aircraft with the same performance capabilities are used, the red side uses an F-16 fighter with *Missile R*, and the blue side uses an Su-27 fighter with *Missile A*. The model conditions are input, and simulations are run through the system interface, as shown in the Figure 11.

TABLE 9. Initial conditions for the enemy aircraft.

	***R*(Red)**	***B*(Blue)**
$x_0^i.m$	10000	30000
$y_0^i.m$	0	-1000
$h_0^i.m$	10000	0
$\chi_0^i.\deg$	100	250
$\gamma_0^i.\deg$	0	20
$v_0^i.m/s$	250	250
Fighter	F-16	Su-27
Missile	R	A

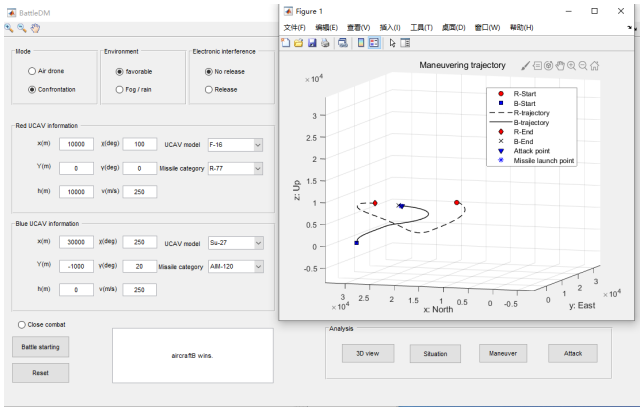

FIGURE 11. Simulation interface and confrontation maneuvering trajectory.

Based on the confrontation simulation, Table 6 and Table 9 show that the aircraft and missile performance levels for the blue side are superior to those for the red side. The simulation results show that compared to the red side, the blue side completes the missile kill process more quickly in the confrontation. Figure 12(a) shows the change in the situation domain for the red side, which had an initial situational advantage, in the confrontation process. To obtain the target information as soon as possible, the red side quickly adjusts course, points the aircraft nose at the target, and increases its speed to keep the target within the radar detection area. The maneuver changes are shown in Figure 12(b).

The performance of the blue side aircraft is better than that of the red side aircraft. Figure 13(a) and Figure 13(b) show the changes in the seeking advantage of the blue side achieved through climbing and other maneuvers. The scenario gradually shifts from an information assurance situation to an attack situation, and the red side is constantly suppressed in the attack situation. At 63 s in the simulation, the accumulated advantage of the blue side allows the aircraft to enter an attack situation. The red side aircraft uses a right turn maneuver to avoid the pursuit of the blue side and ensure that it does not enter the range of the blue missile; however, the initial red advantage is gradually lost due to the inferior performance of the aircraft.

At 141 s, the blue side enters the attack stage, Figure 12(c) and Figure 13(c) show the missile launch times and kill probabilities of the two aircraft. At 169 s in the simulation, the blue side enters the launching state due to its equipment advantages, forcing the red side to enter an attack defense state. A missile is launched at 173 seconds by the blue side, prior to missile launch by the red side. The simulation results indicate that the blue side completes the kill tasks, with a final

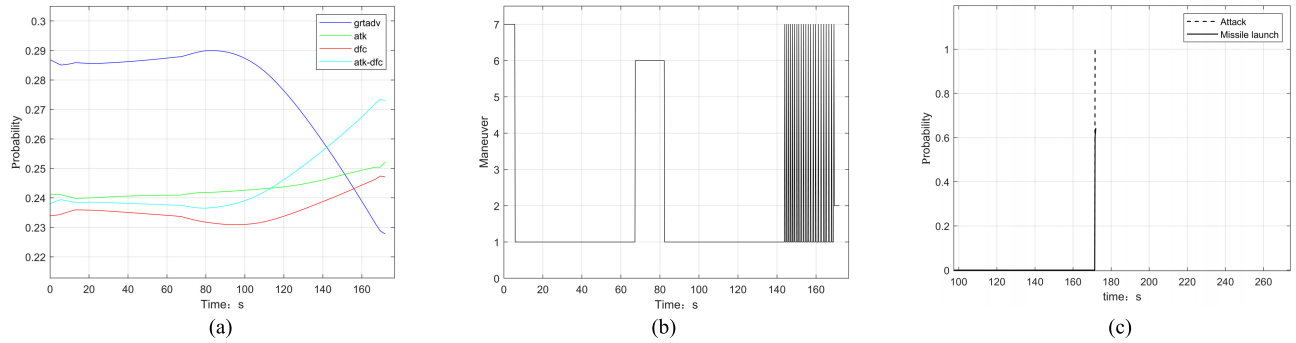

FIGURE 12. Simulation results of Red UCAV.

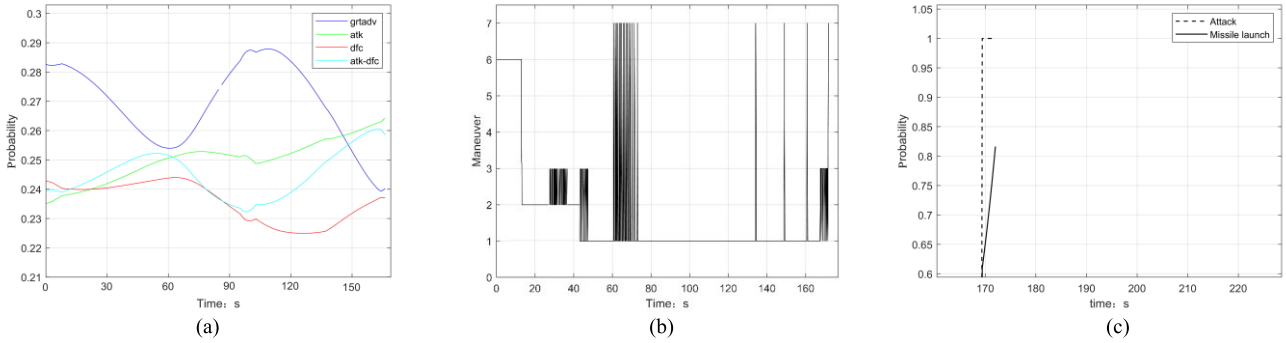

FIGURE 13. Simulation results of Blue UCAV.

kill benefit of 0.643434 for the red side and 0.816282 for the blue side.

Through the simulation experiment involving BVR air combat confrontation, it is verified that the situation assessment model and the maneuver decision model can effectively establish an attack strategy, provide advantages in air combat confrontations, and reflect real air combat confrontation situations.

3) CONTRIBUTION ANALYSIS

By establishing a reasonable countermeasure simulation model, we can calculate the contributions of the relevant airborne equipment types and other influential factors. To calculate the contribution of *Missile A* to the selected fighter in the attack mission, a simulation is conducted by replacing *Missile R* with *Missile A*.

Figure 14 shows that the simulation results are similar for both aircraft. Initially both sides are seeking to gain a positioning advantage in space. Due to the relatively long distance between the two sides, the selected aircraft has enough time to compensate for the disadvantage in aircraft performance, and a maneuver decision is used to achieve a position advantage. At 168 s in the simulation, both sides launch missiles simultaneously, and the kill benefits reach the established threshold; therefore, the simulation is complete. The results indicate that the kill benefit is 0.804910 for both

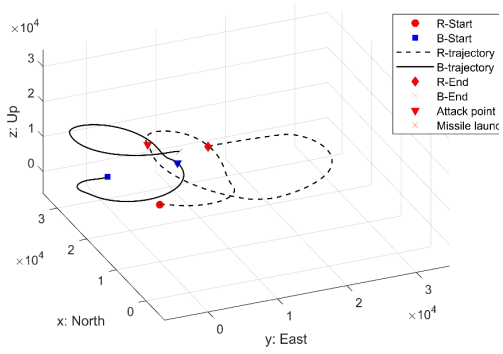

FIGURE 14. Maneuvering trajectory when Missile R is replaced with Missile A.

sides. The contribution of *Missile A* to the aircraft weaponry system can be calculated from (1) as

$$con_{M_A} = \frac{E_{M_A} - E_{M_R}}{E_{M_R}} \times 100\% = 25.09\% \tag{26}$$

The equipment contribution value has a strong correspondence with the countermeasure environment. Taking the environment interference as an example, the radar detection range and missile attack range will be reduced in foggy days. Adding environment interference in the previous simulation, the simulation result in a kill benefit of 0. 0.644802 for red

side and 0.817584 for the blue side when missile a is not replaced, and the kill benefit is 0.806994 for both side after replacing missiles. At this time, the contribution of the missile to the equipment system is 25.15% by calculation. Therefore, the analysis and utilization of equipment contribution depends on the requirements of aircraft mission. According to different mission indicators, the most suitable equipment can be selected based on the contribution.

Moreover, based on the constructed confrontation system, we can calculate the contribution of each equipment types in the weaponry system in the context of the target, such as in the original simulation scenario. Our aircraft has the ability to provide active interference, and the new simulation results show that the obtained kill benefit is 0.763403, while that for the blue side is 0.821523. Thus, the survival and attack capabilities of the red aircraft have significantly improved, and the contribution of active interference equipment is

$$con_{I_A} = \frac{E_{I_A} - E_{non\text{-}I_A}}{E_{non\text{-}I_A}} \times 100\% = 18.65\%. \quad (27)$$

V. CONCLUSION

Due to the uniqueness of the contribution assessment, the calculation results of the contribution degree are effective under the same operational conditions, including the environment, aircraft and airborne equipment. When the influential factors other than the target equipment change, the contribution of the calculation results cannot effectively reflect the contribution of the equipment. Therefore, in the countermeasure simulation, the contribution of *Missile A*. is increased from 25.09% to 25.15%, which shows that only *Missile A*. contributes under the conditions of the current combat mission. Therefore, the contribution evaluation of the target equipment needs to be combined with a variety of mission scenarios to give comprehensive results.

To explore the contributions of new equipment types in a system, this paper proposed a method of airborne equipment contribution assessment to determine the R&D value and effectiveness of equipment. Based on influence diagrams and the BVR context, a situation assessment method based on the situation domain is proposed. This approach makes environmental representations in air combat maneuver decision making more realistic, and battlefield information can be comprehensively used.

Considering the large data volume and low computational efficiency in air combat, based on the rolling horizon theory, a maneuver decision model for fighters in BVR air combat is established, and a corresponding killing benefit calculation method is proposed. The simulation results show that the model can effectively simulate the BVR environment. The calculation method fully considers the diversity and relevance of equipment, improves the authenticity and accuracy of contribution calculations from multiple dimensions, such as system construction, mission support, and maneuver simulation, and achieves the preliminary transformation from static analysis to dynamic analysis.

Due to data and time limitations, this paper does not expand the base maneuver library or consider additional types of airborne equipment. Considering the weaknesses of the current research, the next step is to optimize the calculation of the influence diagrams, which is particularly important for complex systems. In addition, to achieve standardization among equipment systems, the contribution evaluation perspective will be expanded and extended. The contribution evaluation system will be optimized by first enriching the equipment index system used in the air combat field and then gradually expanding the equipment use scenarios. Additionally, a set of comprehensive methods for the contribution evaluation of equipment will be proposed to effectively provide decision support for the equipment R&D process.

REFERENCES

[1] M. Dorczuk, "Modern weapon systems equipped with stabilization systems: Division, development objectives, and research problems," *Sci. J. Mil. Univ. Land Forces*, vol. 197, no. 3, pp. 651–659, Sep. 2020.

[2] W. Yuan and C. Shengyan, "The thinking of digitization management of weapon equipment development in big data era," in *Proc. IEEE 2nd Int. Conf. Cloud Comput. Big Data Anal. (ICCCBDA)*, Apr. 2017, pp. 166–170.

[3] Y. Chi, J. C. Li, K. W. Yang, and Y. J. Tan, "An equipment offering degree evaluation method for weapon system-of-systems combat network based on operation loop," in *Proc. 22nd Int. Conf. Ind. Eng. Manage.*, 2015, pp. 477–488.

[4] Z. Wang, S. Liu, and Z. Fang, "Research on SoS-GERT network model for equipment system of systems contribution evaluation based on joint operation," *IEEE Syst. J.*, vol. 14, no. 3, pp. 4188–4196, Sep. 2020.

[5] Y. Deng, L. Song, J. Zhou, and J. Wang, "Evaluation and reduction of vulnerability of subway equipment: An integrated framework," *Saf. Sci.*, vol. 103, pp. 172–182, Mar. 2018.

[6] J. Xu, Z. Deng, X. Ren, L. Xu, and D. Liu, "Invulnerability optimization of UAV formation based on super wires adding strategy," *Chaos, Solitons Fractals*, vol. 140, Nov. 2020, Art. no. 110185.

[7] J. Li, D. Zhao, J. Jiang, K. Yang, and Y. Chen, "Capability oriented equipment contribution analysis in temporal combat networks," *IEEE Trans. Syst., Man, Cybern., Syst.*, vol. 51, no. 2, pp. 696–704, Feb. 2021.

[8] H. Yang, F. Liu, and Y. Yan, "A new perspective on evaluation software of contribution rate for weapon equipment system," in *Proc. Int. Conf. Geo-Spatial Knowl. Intell.*, 2017, pp. 305–312.

[9] S. Luo, Y. Li, and Y. Chen, "Application of vague sets and TOPSIS method in the evaluation of integrated equipment system of systems," in *Proc. Int. Conf. Commun. Netw. China*, 2020, pp. 595–612.

[10] B. Lin, D. Song, and Z. Liu, "A model of aircraft support concept evaluation based on DEA and PCA," *J. Syst. Sci. Inf.*, vol. 6, no. 6, pp. 563–576, Dec. 2018.

[11] Q. Shi and L. Jian-Xun, "Improved grey correlation analysis for ballistic missile threat assessment," in *Proc. 6th Int. Conf. Inf. Sci. Control Eng. (ICISCE)*, Dec. 2019.

[12] Y. F. Dong, X. P. Wu, and G. M. Qu, "The improved grey relation model for combined operational effectiveness evaluation of fighters," *Flight Dyn.*, vol. 35, no. 2, pp. 92–96, 2017.

[13] P. Dong and Q. Daguo, "Evaluation of contribution rate of weapon equipment system of systems capability based on conditional evidential network," in *Proc. 8th IEEE Int. Conf. Softw. Eng. Service Sci. (ICSESS)*, Nov. 2017, pp. 459–463.

[14] M. Musharraf, J. Smith, F. Khan, B. Veitch, and S. MacKinnon, "Assessing offshore emergency evacuation behavior in a virtual environment using a Bayesian network approach," *Rel. Eng. Syst. Saf.*, vol. 152, pp. 28–37, Aug. 2016.

[15] Y. H. Gu and Z. H. Cheng, "Effectiveness evaluation of wartime equipment maintenance support based on Bayesian network," *Ordnance Ind. Automat.*, vol. 38, no. 10, pp. 80–82, 2019.

[16] W. Xia, X. Liu, S. Meng, and J. Fan, "Efficiency evaluation research of missile weapon system based on the ADC–model," in *Proc. 6th Int. Conf. Mach., Mater., Environ., Biotechnol. Comput.*, 2016, pp. 1227–1236.

[17] N. Zhang, X. Wang, X. Wang, and Z. Wu, "Analysis on the operational effectiveness of certain landmine based on the AHP-ADC combination model of computing," in *Proc. Int. Conf. Intell. Comput., Commun. Devices*. Singapore: Springer, 2019.
[18] J. Shan and Q. Liu, "Analysis of the impact of battlefield environment on military operation effectiveness using fuzzy influence diagram," *Int. J. Fuzzy Syst.*, vol. 21, no. 6, pp. 1882–1893, Sep. 2019.
[19] F. J. Díez, M. Yebra, I. Bermejo, M. A. Palacios-Alonso, M. A. Calleja, M. Luque, and J. Pérez-Martín, "Markov influence diagrams: A graphical tool for cost-effectiveness analysis," *Med. Decis. Making*, vol. 37, no. 2, pp. 183–195, Feb. 2017.
[20] A. Janjic, "Distribution network risk assessment using multicriteria fuzzy influence diagram," *Adv. Fuzzy Syst.*, vol. 2018, pp. 1–10, Sep. 2018.
[21] H. Zheng, Y. Deng, and Y. Hu, "Fuzzy evidential influence diagram and its evaluation algorithm," *Knowl.-Based Syst.*, vol. 131, pp. 28–45, Sep. 2017.
[22] K. Ummah, H. Setiadi, H. M. Pasaribu, and D. Anandito, "A simple fight decision support system for BVR air combat using fuzzy logic algorithm," *Int. J. Aviation Sci. Eng.*, vol. 1, no. 1, pp. 1–5, Dec. 2020.
[23] D. Hu, R. Yang, J. Zuo, Z. Zhang, J. Wu, and Y. Wang, "Application of deep reinforcement learning in maneuver planning of beyond-visual-range air combat," *IEEE Access*, vol. 9, pp. 32282–32297, 2021.
[24] K. Zhao and C. Huang, "Air combat situation assessment for UAV based on improved decision tree," in *Proc. 30th China Conf. Control Decision Making*, Jun. 2018, pp. 1772–1776.
[25] P. Qian, D. Zhou, J. Huang, and X. Lv, "Maneuver decision for cooperative close-range air combat based on state predicted influence diagram," in *Proc. IEEE Int. Conf. Inf. Automat.*, Jul. 2017, pp. 726–731.
[26] J. Poropudas and V. Kai, "Analyzing air combat simulation results with dynamic Bayesian networks," in *Proc. Winter Simul. Conf.*, Dec. 2007, pp. 1370–1377.
[27] W. H. Wu, S. Y. Zhou, L. Gao, and J. T. Liu, "Improvements of situation assessment for beyond-visual-range air combat based on missile launching envelope analysis," *Syst. Eng. Electron.*, vol. 33, no. 12, pp. 2679–2685, 2011.
[28] H. Y. Liu, Y. Zhang, and S. Li, "Simulation and effectiveness analysis on one versus one beyond visual range air combat," in *Proc. MATEC Web Conf.*, vol. 151, 2018, p. 05001.
[29] Y. Gao and J. W. Xiang, "New threat assessment non-parameter model in beyond-visual-range air combat," *J. Syst. Simul.*, vol. 18, no. 9, pp. 2570–2572, 2592, 2006.
[30] F. Neuman, "Methodology for determination and use of the no-escape envelope of an air-to-air-missile," in *Proc. Guid., Navigat. Control Conf.*, Aug. 1988, pp. 707–722.
[31] Y. Hui, Y. Nan, S. Chen, Q. Ding, and S. Wu, "Dynamic attack zone of air-to-air missile after being launched in random wind field," *Chin. J. Aeronaut.*, vol. 28, no. 5, pp. 1519–1528, Oct. 2015.
[32] H. H. You, Q. S. Han, M. J. Yu, and H. M. Ji, "A method to solve the unreachable zone of mid-range air-to-air missile," in *Proc. IEEE 2nd Int. Conf. Electron. Inf. Commun. Technol. (ICEICT)*, Jan. 2019, pp. 649–654.
[33] Y. Xu, Y. F. Ding, and Z. Y. Yan, "Jamming effectiveness evaluation based on radar detection range," *Radar Sci. Technol.*, vol. 9, no. 2, pp. 104–108, 2011.
[34] P. J. F. Lucas, "Certainty-factor-like structures in Bayesian belief networks," *Knowl.-Based Syst.*, vol. 14, no. 7, pp. 327–335, Nov. 2001.
[35] C. Q. Huang, D. Kangsheng, H. Hanqiao, T. Shangqin, and Z. Zhuoran, "Autonomous air combat maneuver decision using Bayesian inference and moving horizon optimization," *J. Syst. Eng. Electron.*, vol. 29, no. 1, pp. 86–97, Feb. 2018.
[36] J. Li, R. Zhang, and Y. Yang, "Multi-AUV autonomous task planning based on the scroll time domain quantum bee colony optimization algorithm in uncertain environment," *PLoS ONE*, vol. 12, no. 11, Nov. 2017, Art. no. e0188291.
[37] M. S. Lewis, "A piloted simulation of one-on-one helicopter air combat in low level flight," *J. Amer. Helicopter Soc.*, vol. 31, no. 2, pp. 19–26, Apr. 1985.

HANCHEN LU was born in Beijing, China, in 1991. He received the bachelor's and master's degrees in navigation guidance and control from Beihang University, China, in 2013 and 2016, respectively. He is currently pursuing the Ph.D. degree in management science and engineering with Harbin Engineering University, China. His research interests include equipment contribution analysis and complex system decision making.

BOYI WU is currently a Professor with Harbin Engineering University, serving as the General Manager Assistant for CIECC, and the General Manager with High-Tech Consultation Center Company Ltd. He has served as the Academic Evaluation Leader for the Expert Academic Committee, CIECC, and the Director of the National E-Government Simulation and Modeling Engineering Laboratory, Harbin Engineering University. He has participated in more than 5,000 planning researches, thematic researches, and other project evaluation and demonstration. He has undertaken dozens of major national projects. His research interests include project proof and evaluation, investment planning, planning research, and policy research. He is a member of Chinese Society of Administrative Management.

JUNQING CHEN received the bachelor's degree in English from Fuzhou University, Fuzhou, China, in 2016. He is currently pursuing the master's and Ph.D. degrees in management science and engineering with Harbin Engineering University, Harbin, China. His research interests include systems engineering, capability assessment, and life cycle asset management.